INFLUENZA

Different genetic barriers for resistance to HA stem antibodies in influenza H3 and H1 viruses

Nicholas C. Wu[1]*, Andrew J. Thompson[2]*, Juhye M. Lee[3,4,5], Wen Su[6], Britni M. Arlian[2], Jia Xie[7], Richard A. Lerner[7,8], Hui-Ling Yen[6], Jesse D. Bloom[3,4,9], Ian A. Wilson[1,8]†

The discovery and characterization of broadly neutralizing human antibodies (bnAbs) to the highly conserved stem region of influenza hemagglutinin (HA) have contributed to considerations of a universal influenza vaccine. However, the potential for resistance to stem bnAbs also needs to be more thoroughly evaluated. Using deep mutational scanning, with a focus on epitope residues, we found that the genetic barrier to resistance to stem bnAbs is low for the H3 subtype but substantially higher for the H1 subtype owing to structural differences in the HA stem. Several strong resistance mutations in H3 can be observed in naturally circulating strains and do not reduce in vitro viral fitness and in vivo pathogenicity. This study highlights a potential challenge for development of a truly universal influenza vaccine.

The major surface antigen of influenza virus, the hemagglutinin (HA), is composed of a highly variable globular head domain that contains the receptor binding site and a highly conserved stem domain that contains the membrane fusion machinery (*1*). The major antigenic sites on HA are located on the globular head (*2*, *3*), which is immunodominant over the stem (*4*). However, most antibodies to the head domain are strain specific, whereas antibodies to the stem are harder to elicit but have considerably more breadth [reviewed in (*5*)]. The isolation, characterization, and structure determination of broadly neutralizing human antibodies (bnAbs) to the HA stem since 2008 (*6*–*9*) have provided insights into immunogen design toward a universal influenza vaccine (*8*, *10*–*13*) and have offered templates for design of small proteins, peptides, and small molecules against influenza virus (*14*–*18*). Several stem bnAbs are also currently in clinical trials (*19*). Therefore, stem bnAbs open up multiple promising avenues to tackle this challenging global health problem.

Resistance mutations can be a major obstacle for antiviral and vaccine development, but the extent to which this is a problem for stem bnAbs is unclear. Several studies have reported difficulty in selecting strong resistance mutations to stem bnAbs even after extensive virus passaging (*20*–*22*), or through deep mutational scanning (*23*), which is a comprehensive and unbiased approach (*24*). Nonetheless, other studies have obtained strong resistance mutations through virus passaging (*6*, *21*, *25*). Here, we systematically compare the extent to which resistance can emerge to stem bnAbs in HAs from the H3 and H1 subtypes that represent the circulating influenza A strains.

Deep mutational scanning of the major HA stem epitope in H3/HK68 HA

CR9114 (*26*) and FI6v3 (*27*) are two prototypic bnAbs that bind the HA stem and represent those with the greatest breadth. Both FI6v3 and CR9114 neutralize group 1 and 2 influenza A viruses (*26*, *27*), and CR9114 further cross-reacts with influenza B HA (*26*). Deep mutational scanning (*24*), which combines saturation mutagenesis and next-generation sequencing, has been applied to study how HA mutations affect influenza viral fitness (*28*–*30*) and to identify viral mutants that are resistant to antibodies against HA (*31*). Here, we used deep mutational scanning of the HA stem of H3N2 A/Hong Kong/1/1968 (H3/HK68) to search for virus resistance mutations to CR9114 and FI6v3. Unlike previous studies that examined the entire HA (*28*–*31*), we focused on eight residues in HA2 (HA0 is cleaved during maturation into HA1 and HA2) of H3/HK68 HA in and around the main stem epitope (the region recognized by an antibody): namely Q42, I45, D46, Q47, I48, N49, L52, and T111 (Fig. 1, A to C). All except T111 are located on HA2 helix A, which is a common target for stem bnAbs. Residues 42, 45, 46, 48, 49, and 52 were chosen because they interact with CR9114 and FI6v3, and residue 47 because it interacts with FI6v3 (Fig. 1, D and E). Completely buried T111 was selected because its mutation in H5 HA enabled escape from CR6261 (*6*), which binds an epitope similar to CR9114 (*9*, *26*).

By considering mutations to all amino acids at each position, we quantified the in vitro viral fitness of 147 of 152 possible single mutants and 6234 of 10,108 possible double mutants across the eight residues of interest in H3/HK68 under five conditions: no antibody, 2 μg/ml CR9114 immunoglobulin G (IgG), 10 μg/ml CR9114 IgG, 0.3 μg/ml FI6v3 IgG, and 2.5 μg/ml FI6v3 IgG (fig. S1). Many mutants have a relative fitness [proxy for replication fitness (*30*)] similar to that of the wild type (WT), which was set as 1 (Fig. 2, A and B), indicating that the HA stem region can tolerate many mutations.

We further quantified the relative resistance (normalized to WT) of each viral mutant by measuring relative fitness (normalized to WT) with or without antibody (fig. S2). Many resistance mutations to CR9114 and FI6v3 were observed (Fig. 2, C and D), and most were located at HA2 residues 42 and 45, which are important in the binding interface with CR9114 and FI6v3 (Fig. 1, D and E). The double mutants also showed high relative resistance if one mutation exhibited high relative resistance even if the other did not (fig. S3A). Consistently, the relative resistance of double mutants can generally be explained by additivity of their corresponding single mutants (fig. S3B). These results demonstrate the prevalence of H3/HK68 resistance mutations to stem bnAbs and identify cross-resistance mutations to both CR9114 and FI6v3, which are encoded by different germline genes and have very different angles of approach to the HA (*5*).

Validation of resistance mutations

We then individually constructed and tested 18 single and 6 double HA mutants of the H3/HK68 virus spanning a range of relative resistance against CR9114 and FI6v3 IgGs (Fig. 3A). The minimum inhibitory concentration (MIC) in a microneutralization assay strongly correlated with the relative resistance from deep mutational scanning (Spearman's rank correlation > 0.8, Fig. 3B), with several mutants showing strong cross-resistance to both CR9114 and FI6v3. For example, the MICs of CR9114 and FI6v3 against mutants I45Y/S/N/F/W were all >100 and ≥20 μg/ml, respectively, compared to 3.1 and 0.2 μg/ml for WT. This validation experiment substantiates our finding that strong resistance mutations are prevalent in H3/HK68.

Natural occurrence of resistance mutations

Next, we explored whether these resistance mutations can be found in naturally circulating strains and identified a few of these strong resistance mutations at low frequency in human H3N2 isolates (*32*), including I45T, I45M, and N49D (Fig. 4A), although most have not

[1]Department of Integrative Structural and Computational Biology, The Scripps Research Institute, La Jolla, CA 92037, USA. [2]Department of Molecular Medicine, The Scripps Research Institute, La Jolla, CA 92037, USA. [3]Basic Sciences Division, Fred Hutchinson Cancer Research Center, Seattle, WA 98109, USA. [4]Department of Genome Sciences, University of Washington, Seattle, WA 98195, USA. [5]Medical Scientist Training Program, University of Washington, Seattle, WA 98195, USA. [6]School of Public Health, Li Ka Shing Faculty of Medicine, The University of Hong Kong, Hong Kong SAR, China. [7]Department of Chemistry, The Scripps Research Institute, La Jolla, CA 92037, USA. [8]The Skaggs Institute for Chemical Biology, The Scripps Research Institute, La Jolla, CA 92037, USA. [9]Howard Hughes Medical Institute, Fred Hutchinson Cancer Research Center, Seattle, WA 98109, USA.

*These authors contributed equally to this work.

†Corresponding author. Email: wilson@scripps.edu

been observed yet in naturally circulating strains. I45T is also observed in human H3N2 isolates sequenced without any passaging (fig. S4A), implying that its presence is not due to a passaging artifact (*33*). Moreover, strong cross-resistance mutation I45F was found in all human H2N2 viruses that circulated from 1957 to 1968 (Fig. 4B and fig. S4B), whereas almost all avian H2N2 viruses have Ile[45] (Fig. 4C). This particular mutation in human H2N2 viruses explains why it is more difficult for some stem bnAbs to bind or neutralize this subtype compared to other subtypes, as found in previous studies (*6*, *26*, *34*). Thus, resistance mutations to stem bnAbs already do indeed occur in circulating strains.

In vivo pathogenicity and escape of resistance mutations

Given their relevance to circulating strains, we further tested the in vivo viral pathogenicity of HA2 mutants I45T, I45M, and I45F. The weight loss profiles in mice after infection by HA2 mutant and WT viruses were comparable (fig. S5), indicating that these resistance mutations do not reduce in vivo pathogenicity. We further demonstrated that I45T, I45M, and I45F could escape in vivo prophylactic protection. Whereas mice infected with WT were completely protected by CR9114 IgG at all tested doses (1, 4, and 10 mg/kg), mutants I45T, I45M, and I45F were lethal even at the highest dose of CR9114 IgG (Fig. 4, D to G).

Resistance mutations decrease affinity to bnAbs

To dissect the resistance mechanism, we tested binding of H3/HK68 I45T, I45M, and I45F recombinant HAs to CR9114 and FI6v3, and to another stem bnAb, 27F3 (*34*), which uses the same V_H1-69 germ line as CR9114 and similarly neutralizes group 1 and 2 influenza A viruses. Binding (dissociation constant K_d) of CR9114 Fab, CR9114 IgG, 27F3 Fab, 27F3 IgG, and FI6v3 IgG to the HA mutants (Table 1 and fig. S6) was diminished, particularly with I45F, where binding to CR9114 and 27F3 (Fab and IgG) was undetectable. By contrast, binding of these stem Fabs and IgGs to the HA mutant N49T, which did not exhibit resistance against CR9114 and FI6v3 (Figs. 2C and 3A), was comparable to that of the WT (Table 1). As a control, we also tested binding of bnAb S139/1 that targets the receptor binding site far from the stem epitope (*35*, *36*). S139/1 IgG affinities for those HA mutants (K_d = 1.8 to 3.1 nM) were similar to that of the WT (K_d = 2.1 nM). Thus, virus resistance to stem bnAbs correlated with a decrease in binding affinity for the mutant HAs.

To evaluate the structural basis of the resistance, we determined crystal structures of

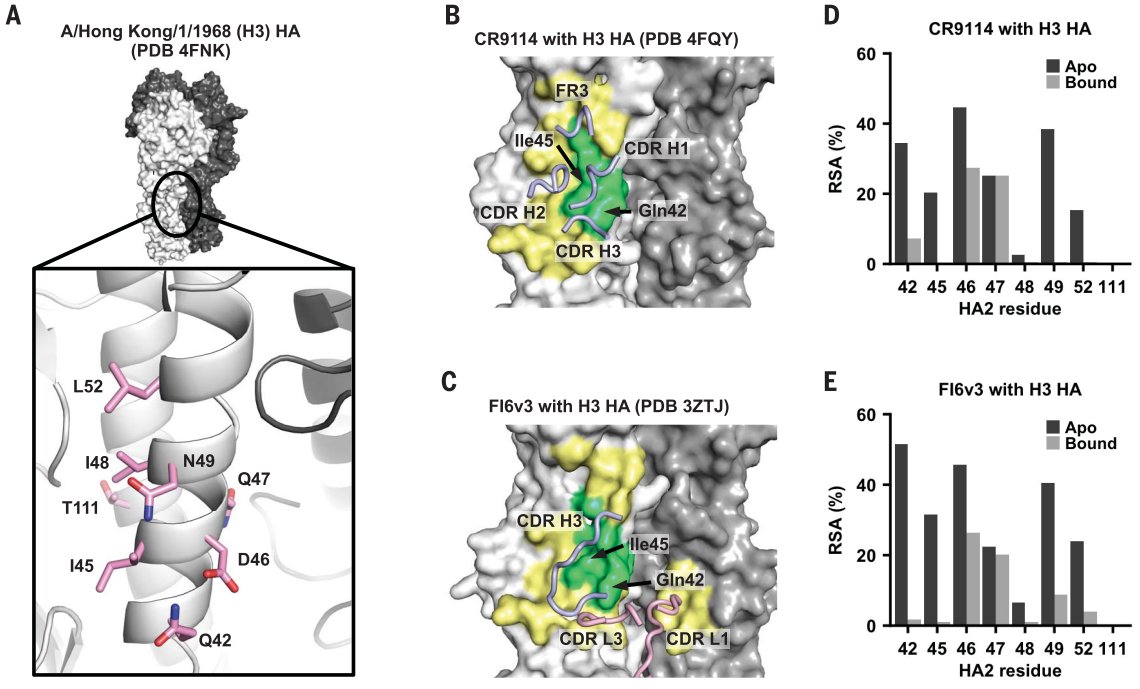

Fig. 1. Epitopes of broadly neutralizing antibodies to the HA stem. (**A**) The location of residues of interest in this study on the HA structures. All residues of interest are on HA2. One protomer of the trimer is shown in light gray and the other two protomers in dark gray, and a detailed view of the location of the residues of interest is shown in the inset. (**B** and **C**) Epitopes of (B) CR9114 Fab in complex with H3 HA (PDB 4FQY) (*26*) and (C) FI6v3 in complex with H3 HA (PDB 3ZTJ) (*27*) are colored in yellow and green, with residues of interest colored in green. The arrows indicate the positions of HA2 residues 42 and 45, which are in the center of the bnAb epitopes. Antibody paratopes (CDRs and FR regions) are shown in tube representation and labeled accordingly. Blue, heavy chain; pink, light chain. (**D** and **E**) The relative solvent accessibility (RSA) of each residue of interest is shown. Black bar, apo form; gray bar, Fab-bound form.

Table 1. Binding affinity of IgGs and Fabs against HAs of WT and different H3/HK68 HA2 mutants. n.b., no binding.

K_d (nM)	WT	HA2-I45T	HA2-I45M	HA2-I45F	HA2-N49T
CR9114 Fab	43.2 ± 0.4	779.6 ± 50.0	319.1 ± 12.1	n.b.	11.3 ± 0.4
27F3 Fab	122.6 ± 3.0	n.b.	n.b.	n.b.	105.0 ± 1.0
CR9114 IgG	<0.1	164.8 ± 2.3	75.0 ± 1.0	n.b.	<0.1
27F3 IgG	1.7 ± 0.1	n.b.	n.b.	n.b.	1.9 ± 0.9
FI6v3 IgG	<0.1	7.8 ± 0.2	6.7 ± 0.1	62.0 ± 0.2	<0.1
S139/1 IgG	2.1 ± 0.1	3.1 ± 0.3	1.9 ± 0.1	1.8 ± 0.1	2.8 ± 0.1

HAs with HA2 mutations I45T, I45M, and I45F to 2.1 to 2.5 Å resolutions (table S1 and fig. S7A). Compared to WT (Ile[45]), the shorter side chain of I45T would create a void when CR9114 is bound (fig. S7B) that would be energetically unfavorable. By contrast, the longer flexible side chain of I45M would likely clash with CR9114 (fig. S7B), but CR9114 can still bind the I45M mutant, albeit with much lower affinity than WT (Table 1). The I45F mutant, however, would clash more severely with CR9114, and no binding was detected (Table 1 and fig. S7B). Similar observations for FI6v3 (fig. S7C) explain the sensitivity of CR9114 and FI6v3 to mutations at HA2 residue 45.

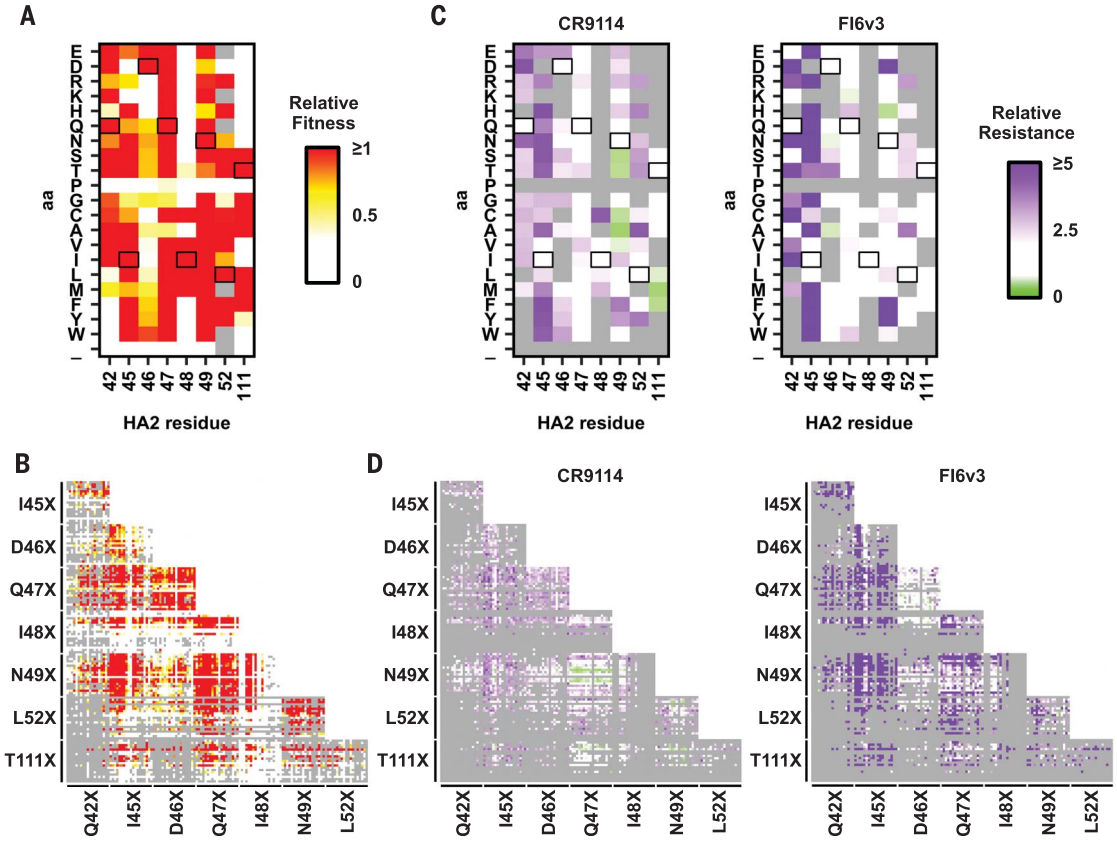

Fig. 2. Fitness and resistance profile of H3/HK68 HA2 single and double viral mutants. (**A** and **B**) On the basis of the deep mutational scanning experiment, the relative fitness of (A) single and (B) double mutants is shown with WT set as 1. In (A) and (B), mutants with a next-generation sequencing read count of less than 20 from the plasmid mutant library are excluded and shown as gray. (**C** and **D**) Relative resistance for (C) each single and (D) each double mutant against 10 μg/ml CR9114 antibody or 2.5 μg/ml FI6v3 antibody is shown. Relative resistance for WT is set as 1. In (C) and (D), mutants with a relative fitness of less than 0.5 are shown as gray. Residues that correspond to the WT sequence are boxed. In (B) and (D), each color point in the heatmap represents a double mutant. Of note, some mutants with an increased sensitivity to antibody are shown in green on the relative resistance color scale. Abbreviations for the amino acid residues are as follows: A, Ala; C, Cys; D, Asp; E, Glu; F, Phe; G, Gly; H, His; I, Ile; K, Lys; L, Leu; M, Met; N, Asn; P, Pro; Q, Gln; R, Arg; S, Ser; T, Thr; V, Val; W, Trp; and Y, Tyr.

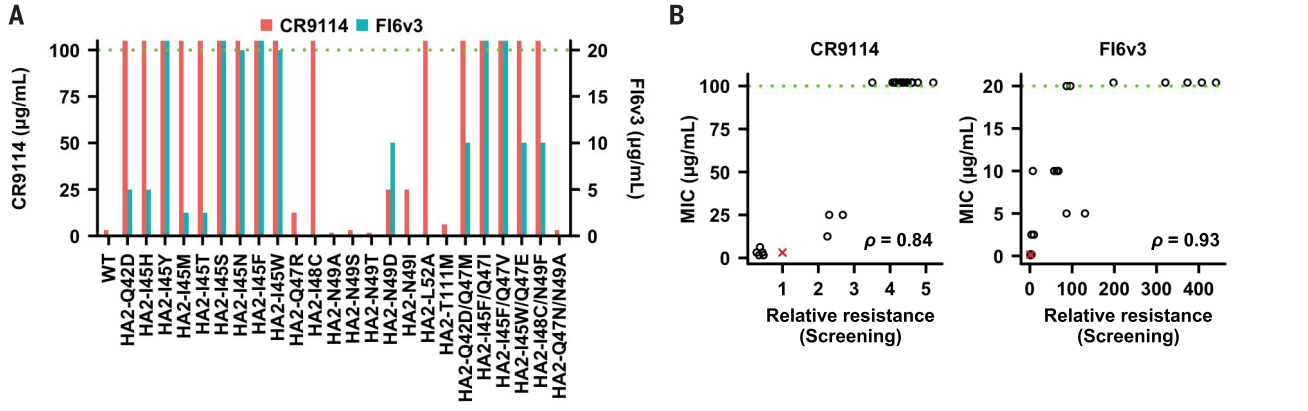

Fig. 3. Characterization of antibody-resistant mutants. (**A**) The minimum inhibitory concentration (MIC) of CR9114 and FI6v3 to individual viral mutants is shown. The MIC of CR9114 is in red and represented by the *y* axis on the left. The MIC of FI6v3 is in blue and represented by the *y* axis on the right. (**B**) The Spearman's rank correlations (ρ) between the MIC measured from individual mutants and the relative resistance (against 10 μg/ml CR9114 antibody or 2.5 μg/ml FI6v3 antibody) computed from the deep mutational scanning experiment (screening) are shown. The green dashed line represents the upper detection limit in (A) and (B). Wild type is represented by the red "X".

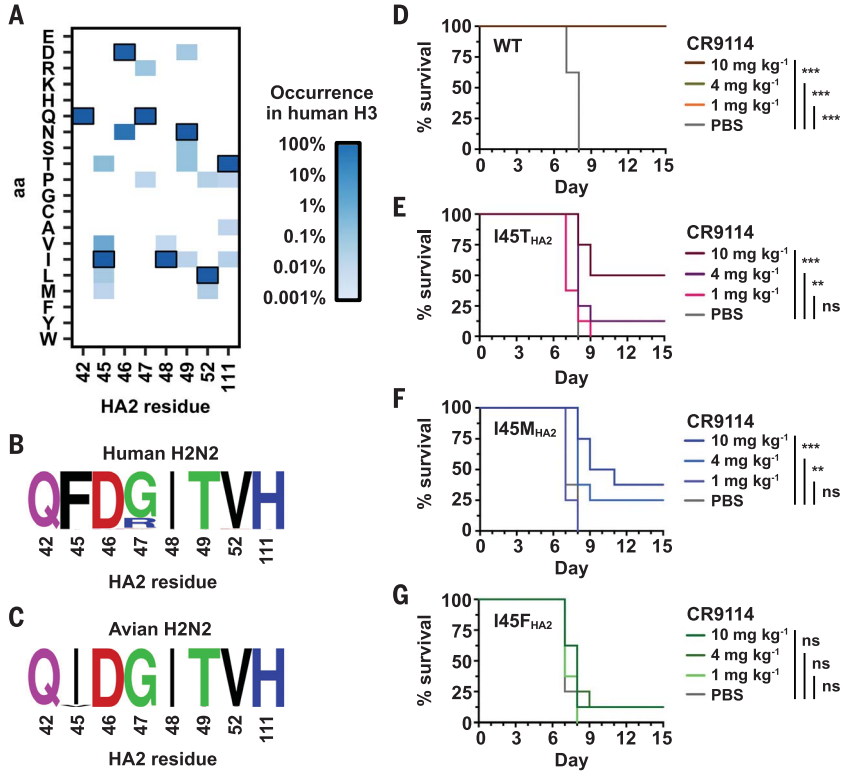

Fig. 4. In vivo characterization and natural occurrence of antibody-resistant mutants. (**A**) The natural occurrence frequencies of different amino acid variants at the residues of interest in human H3 HAs are shown as a heatmap. (**B** and **C**) The natural occurrence frequencies of different amino acid variants at the residues of interest in (B) human H2N2 HA or (C) avian H2N2 HA are shown as sequence logos. (**D** to **G**) Prophylactic protection experiments were performed with different doses of CR9114 against (D) WT, (E) HA2 I45T mutant, (F) HA2 I45M mutant, and (G) HA2 I45F mutant. Recombinant H3/HK68 (7:1 on H1/PR8 backbone) viruses were used. Lethal doses [25 median lethal dose (MLD_{50})] of WT or mutant viruses were used. Kaplan-Meier survival curves are shown. Paired analysis of each treatment group, relative to control, was conducted using Log-rank (Mantel-Cox) tests. ***$P \leq 0.001$; **$P \leq 0.01$; ns (not significant), $P > 0.05$.

Resistance to HA stem bnAbs is subtype specific

We further examined whether mutations that conferred strong resistance in H3/HK68 would have the same phenotypes in other H3 strains. Consequently, we examined I45T, I45M, and I45F mutations on H3N2 A/Wuhan/359/95 (H3/Wuhan95) virus. These mutants had WT-like titers after viral rescue and passaging (fig. S8A), showed a plaque size similar to that of WT (fig. S8B), conferred strong resistance to FI6v3 (fig. S8, C and D), and, therefore, have similar phenotypes in H3/HK68 and H3/Wuhan95 viruses. This result led us to hypothesize that strong resistance mutants to stem bnAbs are readily attainable in human H3 strains that span a wide range of years, as well as explore whether the same phenomenon can be observed in the H1 subtype, which is the other currently circulating influenza A subtype in the human population.

In contrast to our findings for H3/HK68, deep mutational scanning found that resistance mutants of H1N1 A/WSN/33 (H1/WSN) virus to FI6v3 were rare and had only very small effects (*23*). To further investigate the difference between H3 and H1 strains, we performed four additional deep mutational scanning experiments—three with H1N1 strains, namely A/Solomon Islands/3/2006 (H1/SI06) against FI6v3, A/Michigan/45/2015 (H1/Mich15) against FI6v3, and H1/WSN against CR9114; and one with H3N2 strain A/Perth/16/2009 (H3/Perth09) against FI6v3. The H1/SI06 and H1/Mich15 HA mutant virus libraries contain all possible single substitutions at HA2 residues 42, 45, 46, 47, 48, 49, 52, and 111, whereas H1/WSN and H3/Perth09 HA mutant virus libraries both contain all possible single substitutions across the entire HA and were constructed previously (*37*, *38*). We also analyzed the previously published dataset on H1/WSN against FI6v3 (*23*).

To compare H1/SI06, H1/Mich15, H1/WSN, and H3/Perth09 to H3/HK68, we computed the relative resistance of mutations at HA2 residues 42, 45, 46, 47, 48, 49, 52, and 111 (Fig. 5, A to E). Similar to H3/HK68, resistance mutations are highly prevalent in H3/Perth09 (Fig. 5C). Conversely, resistance mutations were rare in H1/SI06, H1/Mich15, and H1/WSN (Fig. 5, A to E). We further calculated the fraction surviving (*23*) for each viral mutant across the entire H1/WSN and H3/Perth09 HAs during antibody selection. Fraction surviving is a quantitative measure for the resistance and is normalized across deep mutational scanning experiments (*23*). For example, fraction surviving values of 1, 0.5, and 0.1 indicate that the replication fitness in the presence of antibody selection is 100, 50, and 10% of that without antibody selection. The fraction surviving values of H1/WSN mutants against CR9114 were all very small, similar to previous observations of H1/WSN against FI6v3 (Fig. 5F and fig. S10). In stark contrast, many mutants of H3/Perth09 were identified with a large fraction surviving value (Fig. 5F). Consistent with the relative resistance profile of H3/HK68 (Fig. 2C), a number of H3/Perth09 mutants with a large fraction surviving value were found at HA2 residues 42 and 45 (Fig. 5F and fig. S11A). Moreover, mutations at HA2 residue 53, which were not examined in H3/HK68 (Fig. 2), had high fraction surviving values in H3/Perth09 against FI6v3 (fig. S11, A and B). In H3 HA, mutation of HA2 residue 53 would abolish a hydrogen bond to FI6v3 (fig. S11B). Together, these results suggest that the prevalence of resistance mutations to stem bnAbs is a general phenomenon for the H3 subtype but not the H1 subtype.

Subtype-specific differences in the HA stem

We next aimed to elucidate the mechanism that underlies the lower genetic barrier to resistance to stem bnAbs in H3 HA as compared to H1 HA. Many mutations at HA2 residue 45 have a high fitness cost in H1/SI06 (fig. S9A), which can increase the genetic barrier to resistance. However, most mutations at HA2 residue 45 have no fitness cost in H1/Mich15. In addition, the mutational fitness profiles of H1/SI06 and H1/Mich15 (fig. S9, A and B) show that many mutations can be tolerated in the HA stem, similar to H3/HK68 (Fig. 2A and fig. S9, C to F). Thus, the difference in genetic barrier to resistance to stem bnAbs between H1 and H3 subtypes cannot be fully explained by their ability to tolerate mutations (i.e., fitness cost of mutations).

We therefore further compared the structures of FI6v3 in complexes with H1 HA and

H3 HA (*27*). The orientation of Tyr100c [Kabat numbering (*39*)] on the third complementarity determining region of the antibody heavy chain (CDR H3) of FI6v3 differs when binding to H1 or H3 HAs (Fig. 5G). The position of HA2 Ile^{45} also differs between H1 and H3 HAs when FI6v3 is bound. As a result, Tyr100c of FI6v3 packs tighter to HA2 Ile^{45} of H3 than of H1 HA. Thus, a bulkier substitution at residue 45 of HA2 will disrupt binding of FI6v3 to H3 HA more than to H1 HA. Therefore, the low genetic barrier to resistance to stem bnAbs in the H3 subtype can be partly attributed to both high mutational tolerance in the HA stem and subtype-specific structural features, but it is likely that the latter plays a more critical role in determining subtype-specific differences. Although a number of subtype-specific structural features are known in the stem region (*40*), how they influence the genetic barriers for resistance to stem bnAbs remains to be addressed in future studies.

Implications for escape from a universal vaccine or therapeutic stem bnAbs

Prior studies of influenza bnAbs have not considered whether different subtypes might have different abilities to generate resistance mutations against bnAbs. We find here that H3 HA has a much lower genetic barrier to resistance to two of the broadest bnAbs, CR9114 and FI6v3, as compared to H1 HA, consistent with reports of strong resistance to other human HA stem antibodies in the H3 subtype (*21*, *25*, *41*) versus none (*21*) to weak resistance (*22*, *23*) in the H1 subtype. Therefore, it may be easier for stem bnAbs to suppress H1 rather than H3 subtype viruses.

Because the HA stem is immunosubdominant to the head domain, immunological pressure on the HA stem may not yet be sufficient to affect the evolution of circulating human viruses (*42*). However, several stem bnAbs are currently in clinical trials (*19*), and some recently developed influenza vaccine immunogens have focused on targeting the HA stem (*5*, *8*). If stem bnAbs begin to be distributed on a global scale, the immunological pressure on the HA stem will increase. Our findings here indicate that resistance mutations could emerge, at least in the H3 subtype.

Although resistance mutations to stem bnAbs are still rare in currently circulating influenza strains (Fig. 4A), it is important to evaluate the potential impact of such mutations, because many vaccine strategies aim to elicit anti-stem antibodies. We could not overcome some key resistance mutations (I45T, I45M, and I45F) by in vitro evolution of CR9114 (fig. S12). Nonetheless, the best strategy to prevent or overcome such resistance may involve delivery or elicitation of a combination of antibodies with different resistance profiles. The discovery and characterization of bnAbs with

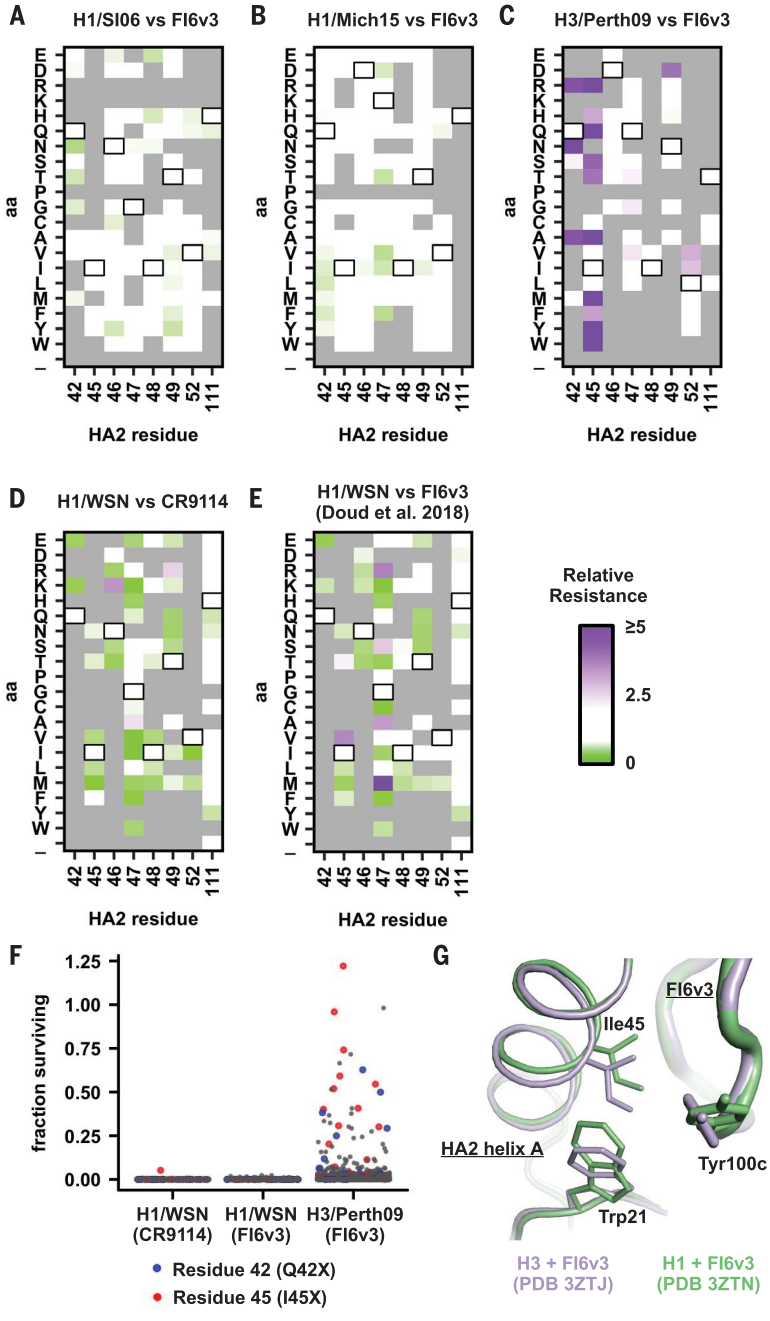

Fig. 5. Relative resistance profile of single mutants in multiple strains of influenza virus. (**A** to **E**) Relative resistance is measured for each single viral mutant at HA2 residues 42, 45, 46, 47, 48, 49, 52, and 111 of (A) H1/SI06 against 300 ng/ml FI6v3 antibody, (**B**) H1/Mich15 against 300 ng/ml FI6v3 antibody, (**C**) H1/WSN against 100 ng/ml CR9114 antibody, (**D**) H1/WSN against 200 ng/ml FI6v3 antibody [data are from (*23*)], and (**E**) H3/Perth09 against 15 μg/ml FI6v3 antibody. Relative resistance for WT is set as 1. Mutants with a relative fitness of less than 0.5 are excluded and shown as gray. Residues that correspond to the WT sequence are boxed. (**F**) Fraction surviving for all single mutants across the HA protein is shown. Each data point represents one mutant. Fraction surviving was computed as previously described (*23*). Assuming no antibody-mediated enhancement of virus replication, the theoretical upper limit for the fraction surviving is 1, which indicates that the replication fitness is the same with and without antibody selection (in practice, fraction surviving values slightly >1 can sometimes be obtained because of the experimental error in quantitative polymerase chain reaction and next-generation sequencing). Data for H1/WSN against FI6v3 were from a previous study (*23*). Data points that represent mutations at residues 42 and 45 are colored in blue and red, respectively, and mutations at other residues are in gray. (**G**) The crystal structures of H3 HA in complex with FI6v3 (PDB 3ZTJ) (*27*) and H1 HA in complex with FI6v3 (PDB 3ZTN) (*27*) were compared by aligning their heavy-chain variable domains. Because the structure of CR9114 with H1 HA is not available, a similar analysis was not performed on CR9114.

different escape profiles will continue to be key to broadening our arsenal against influenza virus. For example, human H2N2 virus, which carries a Phe at HA2 residue 45, often has low reactivity with stem bnAbs (*6*, *26*, *27*, *34*, *43*), although a few can have high potency against human H2N2 (*44*–*46*). Future studies on anti-stem responses against human H2N2 and emerging viruses, such as H5N1 and H7N9, may provide further insights into how to overcome potential resistance should immune pressure become focused on the HA stem.

REFERENCES AND NOTES

1. I. A. Wilson, J. J. Skehel, D. C. Wiley, *Nature* **289**, 366–373 (1981).
2. D. C. Wiley, I. A. Wilson, J. J. Skehel, *Nature* **289**, 373–378 (1981).
3. A. J. Caton, G. G. Brownlee, J. W. Yewdell, W. Gerhard, *Cell* **31**, 417–427 (1982).
4. F. Krammer, P. Palese, *Nat. Rev. Drug Discov.* **14**, 167–182 (2015).
5. N. C. Wu, I. A. Wilson, *J. Mol. Biol.* **429**, 2694–2709 (2017).
6. M. Throsby *et al*., *PLOS ONE* **3**, e3942 (2008).
7. J. Sui *et al*., *Nat. Struct. Mol. Biol.* **16**, 265–273 (2009).
8. N. C. Wu, I. A. Wilson, *Nat. Struct. Mol. Biol.* **25**, 115–121 (2018).
9. D. C. Ekiert *et al*., *Science* **324**, 246–251 (2009).
10. A. Impagliazzo *et al*., *Science* **349**, 1301–1306 (2015).
11. H. M. Yassine *et al*., *Nat. Med.* **21**, 1065–1070 (2015).
12. S. A. Valkenburg *et al*., *Sci. Rep.* **6**, 22666 (2016).
13. K. S. Corbett *et al*., *mBio* **10**, e02810–e02818 (2019).
14. S. J. Fleishman *et al*., *Science* **332**, 816–821 (2011).
15. T. A. Whitehead *et al*., *Nat. Biotechnol.* **30**, 543–548 (2012).
16. A. Chevalier *et al*., *Nature* **550**, 74–79 (2017).
17. R. U. Kadam *et al*., *Science* **358**, 496–502 (2017).
18. M. J. P. van Dongen *et al*., *Science* **363**, eaar6221 (2019).
19. E. Sparrow, M. Friede, M. Sheikh, S. Torvaldsen, A. T. Newall, *Vaccine* **34**, 5442–5448 (2016).
20. G. Nakamura *et al*., *Cell Host Microbe* **14**, 93–103 (2013).
21. N. Chai *et al*., *PLOS Pathog.* **12**, e1005702 (2016).
22. C. S. Anderson *et al*., *Sci. Rep.* **7**, 14614 (2017).
23. M. B. Doud, J. M. Lee, J. D. Bloom, *Nat. Commun.* **9**, 1386 (2018).
24. D. M. Fowler, S. Fields, *Nat. Methods* **11**, 801–807 (2014).
25. R. H. Friesen *et al*., *Proc. Natl. Acad. Sci. U.S.A.* **111**, 445–450 (2014).
26. C. Dreyfus *et al*., *Science* **337**, 1343–1348 (2012).
27. D. Corti *et al*., *Science* **333**, 850–856 (2011).
28. N. C. Wu *et al*., *Sci. Rep.* **4**, 4942 (2014).
29. B. Thyagarajan, J. D. Bloom, *eLife* **3**, e03300 (2014).
30. N. C. Wu *et al*., *Cell Host Microbe* **21**, 742–753.e8 (2017).
31. M. B. Doud, S. E. Hensley, J. D. Bloom, *PLOS Pathog.* **13**, e1006271 (2017).
32. R. B. Squires *et al*., *Influenza Other Respir. Viruses* **6**, 404–416 (2012).
33. N. C. Wu *et al*., *PLOS Pathog.* **13**, e1006682 (2017).
34. S. Lang *et al*., *Cell Rep.* **20**, 2935–2943 (2017).
35. R. Yoshida *et al*., *PLOS Pathog.* **5**, e1000350 (2009).
36. P. S. Lee *et al*., *Proc. Natl. Acad. Sci. U.S.A.* **109**, 17040–17045 (2012).
37. M. B. Doud, J. D. Bloom, *Viruses* **8**, 155 (2016).
38. J. M. Lee *et al*., *Proc. Natl. Acad. Sci. U.S.A.* **115**, E8276–E8285 (2018).
39. Kabat numbering scheme is commonly used standard for numbering the amino-acid residues in an antibody. Third complementarity-determining region of heavy chain (CDR H3) ranges from residues 95 to 102 in the Kabat numbering scheme. Residues inserted in CDR H3 are numbered with 100a, 100b, 100c, and so on.
40. S. J. Zost, N. C. Wu, S. E. Hensley, I. A. Wilson, *J. Infect. Dis.* **219** (suppl. 1), S38–S45 (2019).
41. D. C. Ekiert *et al*., *Science* **333**, 843–850 (2011).
42. E. Kirkpatrick, X. Qiu, P. C. Wilson, J. Bahl, F. Krammer, *Sci. Rep.* **8**, 10432 (2018).
43. M. G. Joyce *et al*., *Cell* **166**, 609–623 (2016).
44. Y. Okuno, Y. Isegawa, F. Sasao, S. Ueda, *J. Virol.* **67**, 2552–2558 (1993).
45. C. Dreyfus, D. C. Ekiert, I. A. Wilson, *J. Virol.* **87**, 7149–7154 (2013).
46. N. L. Kallewaard *et al*., *Cell* **166**, 596–608 (2016).
47. J. Lee, J. Bloom, jbloomlab/HA_stalkbnAb_MAP: journal submission, Version journal_submission, Zenodo (9 February 2020); https://doi.org/10.5281/zenodo.3660467.
48. N. C. Wu, wchnicholas/HAstemEscape: publication, Version publication, Zenodo (9 February 2020); https://doi.org/10.5281/zenodo.3660739.
49. N. C. Wu, wchnicholas/CR9114mut: publication, Version publication, Zenodo (9 February 2020); https://doi.org/10.5281/zenodo.3660731.

ACKNOWLEDGMENTS

We thank W. Yu and G. Grande for technical support in protein expression; S. Head, J. Ledesma, and P. Natarajan (TSRI Next Generation Sequencing Core and Fred Hutch Genomics Core) for next-generation sequencing; M. Haynes and B. Seegers (TSRI Flow Cytometry Core Facility) for performing FACS; A. Ho, E.-M. Strauch, and B. Graham for insightful discussions; and J. Paulson for his continual support. **Funding:** We acknowledge support from the Bill and Melinda Gates Foundation OPP1170236 (to I.A.W.), NIH K99 AI139445 (to N.C.W.), F30 AI136326 (to J.M.L.), R01 AI127893 (to J.D.B.), R56 AI127371 (to I.A.W.), and R01 AI114730 (to J. C. Paulson) This work was partially supported through an NIAID Collaborative Influenza Vaccine Innovation Centers (CIVIC) contract (75N93019C00051). J.M.L. was supported in part by the Center for Inference and Dynamics of Infectious Diseases (CIDID), funded by NIH U54 GM111274. J.D.B. is an investigator of the Howard Hughes Medical Institute. **Author contributions:** N.C.W., J.M.L., R.A.L., H.-L.Y., J.D.B., and I.A.W. conceived and designed the study. N.C.W. and J.M.L. performed the deep mutational scanning experiments. N.C.W., J.M.L., and J.D.B. performed the computational data analysis. N.C.W. performed the structural analysis and yeast display experiment. N.C.W. and W.S. performed functional characterization of the viral mutants. A.J.T. and B.M.A. performed the in vivo characterization of the viral mutants. N.C.W. and J.X. produced the CR9114 and 27F3 antibodies. J.M.L. produced the FI6v3 antibody. N.C.W. and I.A.W. wrote the paper, and all authors reviewed and edited the paper. **Competing interests:** The authors declare no competing interests. **Data and materials availability:** Raw sequencing data have been submitted to the NIH Short Read Archive under accession numbers BioProject PRJNA510654, PRJNA493101, and PRJNA510700. X-ray coordinates and structure factors are deposited at the RCSB Protein Data Bank under accession codes 6NHP, 6NHQ, and 6NHR. Computer codes and processed data are deposited at Zenodo (*47*–*49*). All other data that support the conclusions are included in the manuscript or supplementary materials. The pHW2000 plasmids encoding the eight genes of A/Wuhan/359/95 (H3N2) virus and HA plasmids containing the HA2 mutations are available for noncommercial use from H.-L.Y. under a material transfer agreement (University of Hong Kong). All other materials are available from I.A.W. on request.

SUPPLEMENTARY MATERIALS

science.sciencemag.org/content/368/6497/1335/suppl/DC1
Materials and Methods
Figs. S1 to S12
Tables S1 to S3
References (*50*–*69*)

View/request a protocol for this paper from *Bio-protocol*.

16 September 2019; accepted 14 April 2020
10.1126/science.aaz5143

Different genetic barriers for resistance to HA stem antibodies in influenza H3 and H1 viruses

Nicholas C. Wu, Andrew J. Thompson, Juhye M. Lee, Wen Su, Britni M. Arlian, Jia Xie, Richard A. Lerner, Hui-Ling Yen, Jesse D. Bloom and Ian A. Wilson

Science **368** (6497), 1335-1340.
DOI: 10.1126/science.aaz5143

Resistance to influenza antibodies

Broadly neutralizing human antibodies (bnAbs) to the stem of hemagglutinin (HA), a trimeric glycoprotein found on the surface of influenza viruses, are valuable therapeutics and can guide the development of universal influenza vaccines. For their use in therapy development, it is important to understand the extent to which HA stem variants with resistance to bnAbs can develop. Wu *et al.* used saturation mutagenesis combined with next-generation sequencing to systematically search for resistance mutations to prototypic bnAbs in two influenza subtypes, H3 and H1. They found that the genetic barrier to resistance to stem bnAbs was low for the H3 subtype but higher for the H1 subtype. The ability of H3 to develop resistance to bnAbs presents a challenge in the development of a universal influenza vaccine.

Science, this issue p. 1335